JOURNAL OF MATERIALS SCIENCE **33** (1998) 4775–4782

Damage probability in laminated glass subjected to low velocity small missile impacts

F. S. JI, L. R. DHARANI*
Department of Mechanical and Aerospace Engineering and Engineering Mechanics, University of Missouri-Rolla, Rolla, MO 65409-0050, USA
E-mail: dharani@umr.edu

R. A. BEHR
Department of Architectural Engineering, The Pennsylvania State University, University Park, PA 16802-1416, USA

The probability of damage at the impact site in the outer glass ply of laminated glass units subjected to low velocity small missile impacts is investigated. A dynamic, non-linear finite element analysis is applied to compute the stress response on impacts. Based on the cumulative damage theory, a damage factor is introduced and related to Weibull's distribution of probability to characterize the probability of damage. In conjunction with the finite element analysis, controlled experiments are conducted to determine the material constants appearing in the damage model and Weibull's distribution of probability. A parametric study involving impact velocity, glass ply thickness and interlayer thickness is presented.

1. Introduction

Laminated glass units consisting of two soda lime glass plies adhered by a polymer interlayer are used for architectural and automotive glazing. Polyvinyl butyryl (PVB) is the industry standard polymeric interlayer because of its excellent adhesive and optical qualities. When subjected to severe dynamic blast pressure or missile impacts, even if laminated glass units break, fragments of broken glass plies still adhere to the interlayer, thereby reducing the possibility of bodily injury and property damage caused by flying glass fragments. Another important characteristic of laminated glass units is that the outer glass ply, when exposed to missile impacts can be fractured, while the inner glass ply remains unfractured. In automotive applications, impacts can be caused, for example, by a small stone thrown from the wheel of a leading vehicle into the windshield of a following vehicle. In architectural applications, windborne debris, such as roof gravel, can be hurled with sufficient velocity to break windows. A study of damage caused by hurricane Alicia which struck Houston, TX in August 1983 confirmed the occurrence of widespread window breakage caused by windborne debris impact [1]. The need for improved impact resistance of architectural glazing is clearly evident.

In order to evaluate the structural behaviour of laminated glass units and use them effectively and safely in building applications, researchers in the fields of materials engineering, civil engineering and engineering mechanics have performed a variety of experimental and theoretical studies. Huntsberger [2] presented a simplified mathematical model to evaluate the adhesive behavior of the PVB interlayer to the glass plies. Behr *et al*. [3] experimentally investigated the behaviour of laminated glass units under uniform lateral pressure and compared the resulting experimental data with numerical results obtained from a theoretical model in which two glass plies were layered (i.e. the glass plies were not adhered to the PVB interlayer). Behr and co-workers [4] performed experiments to study the effects of load duration and interlayer thickness on the behavior of laminated glass units. Vallabhan and co-workers [5] developed a simplified mathematical model for establishing the structural mechanics behaviour of laminated glass units under uniform lateral pressure, in which the effect of the PVB interlayer was ignored. Vallabhan *et al*. [6] presented a sophisticated mathematical model for laterally loaded laminated glass units in which the PVB interlayer simply transferred shear stress while the glass plies were subjected to bending moments and membrane tension. The resulting mathematical model computations were in good agreement with the available experimental data. Flocker and Dharani [7] used a non-linear finite element analysis to model stress wave propagation in laminated glass units subjected to small, low velocity missile impacts. In all of the above studies, only prebreakage behaviour of laminated glass units was investigated.

Other researchers investigated the postbreakage behaviour of laminated glass units. Pantelides and co-workers [8] experimentally investigated the postbreakage behaviour of heat-strengthened laminated glass

*Author for correspondence.

units under wind effects, wherein the breakage was caused by small missile impacts. In their work, the ability of heat-strengthened laminated glass units to withstand small missile impacts without breaking the inner glass ply was evaluated. Behr and Kremer [9] performed experiments to evaluate the performance of laminated glass units under simulated windborne debris impacts. They found that increased interlayer thickness could significantly reduce the observed probability of inner glass ply breakage resulting from small windborne debris impacts. Flocker and Dharani modified a traditional nonlinear finite element code to model outer glass ply fracture [10] and adhesive interlayer debonding [11] in laminated glass units subjected to small, low velocity missile impacts. Behr *et al*. [12] reported an experimental validation of the mechanics-based finite element model of Flocker and Dharani [7] for architectural laminated glass units subjected to low velocity small missile impacts. Dynamic strains predicted by the finite element analysis were found to be in close agreement with those measured with a high speed strain gage data acquisition system.

In the above experimental study [12], it was observed that damage occurs first at the impact site on the exposed surface of the outer glass ply due to large compressive stresses there. As the impact velocity increases, the damaged area may increase in size and finally lead to the formation of a Hertz cone in the outer glass ply. A similar phenomenon was observed by Ball and McKenzie [13] in monolithic glass plates. If the impact velocity of a given windborne missile is sufficiently high, fracture will occur in both the outer and inner glass plies of a laminated glass unit. As a first step towards modelling the failure probability of the inner glass ply, the probability of damage at the impact site on the exposed surface of the outer glass ply of a laminated glass unit subjected to low velocity small missile impacts will be studied in this paper.

This paper describes a rigorous approach based on a dynamic, non-linear finite element method to predict the probability of damage in the outer glass ply. The dynamic non-linear finite element analysis is applied to compute the stress response to missile impacts. Based on the cumulative damage concept which was presented by Tuler and Butcher [14] and Brown [15], a damage factor is introduced and related to Weibull's distribution of damage probability to characterize the probability of damage. In conjunction with the finite element analysis, controlled experiments are conducted to determine the material parameters appearing in the damage model and Weibull's distribution. The numerical approach will be then applied to predict the probability of damage associated with impact velocity, glass ply thickness and interlayer thickness.

2. Formulations

Consider a laminated glass unit consisting of an outer glass ply of thickness h_o and an inner glass ply of thickness h_i adhered to a PVB interlayer of thickness h_{PVB} impacted normal to the outer glass ply surface by a small hard missile modeled as a steel ball of radius R with initial impact velocity V_0, as shown in Fig. 1. Cylindrical coordinates (r, θ, z) with a Lagrangian description of motion are used in this problem. This impact problem is axisymmetric, so normal stresses are independent of the angle θ and the shear stress components $\tau_{r\theta}$ and $\tau_{\theta z}$ vanish.

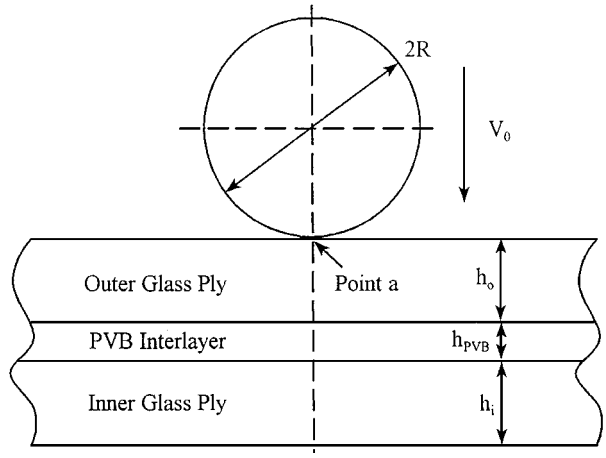

Figure 1 Schematic diagram of a laminated glass subjected to a low-velocity 2 g missile impact.

2.1. Finite element modelling

Following the work of Flocker and Dharani [7], the impact problem is solved numerically using the dynamic non-linear finite element code DYNA2D developed by Whirley and co-workers [16]. The basic equations governing this problem are given by Hallquist [17]. As with most impact formulations, the stress components can be computed as follows

$$\sigma_{ij} = S_{ij} - p\delta_{ij} \tag{1}$$

$$p = -\frac{1}{3}\sigma_{kk} \tag{2}$$

where σ_{ij} are the stress components, S_{ij} are the deviatoric stress components, p is the pressure and δ_{ij} is the Kronecker delta. The usual convention of repeated subscripts implying summation is used.

The glass plies and steel ball are modeled as linear elastic materials. The deviatoric and volumetric behaviours are given by

$$S_{ij} = \left[\frac{E\nu\epsilon_{kk}}{(1+\nu)(1-2\nu)} + p\right]\delta_{ij} + \frac{E\epsilon_{ij}}{(1+\nu)} \tag{3}$$

$$p = -\frac{E\epsilon_{kk}}{3(1-2\nu)} \tag{4}$$

where ϵ_{ij} are the strain components, E is Young's modulus and ν is Poisson's ratio. The PVB interlayer is modelled as a linear visco-elastic material for which the deviatoric stress component is given by

$$S_{ij}(t) = 2\int_0^t G(t-\tau)\dot{e}_{ij}\,\mathrm{d}\tau \tag{5}$$

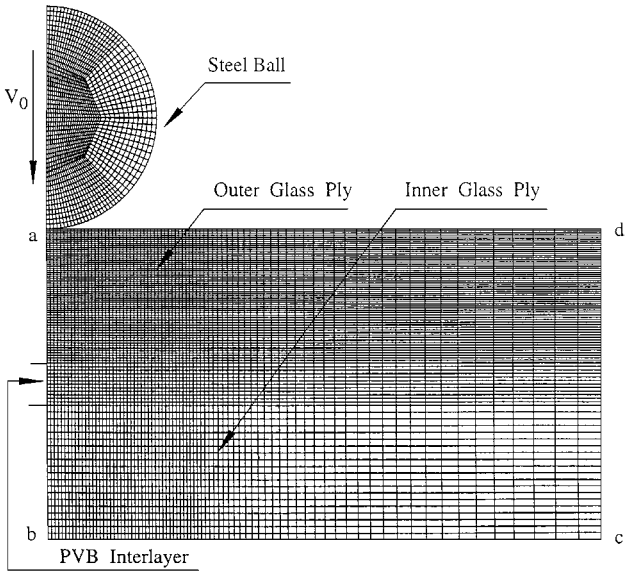

Figure 2 A typical finite element mesh for a laminated glass unit.

where t denotes time, $\dot{e}_{ij}$ is the deviatoric strain rate and $G(t)$ is the stress relaxation modulus, assumed to be of the form

$$G(t) = G_\infty + (G_0 - G_\infty)\mathrm{e}^{-\beta t} \tag{6}$$

where G_∞ is the long time shear modulus, G_0 is the short time shear modulus and β is the decay factor. The volumetric response is elastic, so the pressure p is computed by

$$p = -K\epsilon_{kk} \tag{7}$$

where K is the bulk modulus.

In this finite element analysis, the following constants are used [12]: for the glass plies, $E = 72$ GPa, $\nu = 0.25$, mass density $\rho = 2500\,\mathrm{kg\ m^{-3}}$; for the steel ball, $E = 200$ GPa, $\nu = 0.29$, $\rho = 7800\,\mathrm{kg\ m^{-3}}$, $R = 3.97$ mm; and for the PVB interlayer, $G_0 = 0.33$ GPa, $G_\infty = 0.69$ MPa, $K = 20$ GPa, $\beta = 12.6\,\mathrm{s^{-1}}$ and $\rho = 1100\,\mathrm{kg\ m^{-3}}$. The laminated glass unit and steel ball are discretized using four-noded elements. A typical mesh is illustrated in Fig. 2, which represents, due to the axisymmetric natural of the problem, only half of the actual geometry. The boundaries b–c and a–d are unconstrained while c–d is a so-called "non-reflecting boundary" that is achieved by producing an impedance matching function to cancel incoming stress waves. Non-reflecting boundaries are used to simulate infinite bodies. In this problem, the planar dimensions of laminated glass units are very large compared with their thicknesses and the geometry of the steel ball. Therefore, it is reasonable to assume that c–d is a non-reflecting boundary.

2.2. Glass damage model

For brittle materials such as glass, a maximum stress failure criterion is widely applied to predict material failure. In a dynamic situation, however, the material strength varies as a function of loading duration. Mencik [18] mentioned that the dynamic tensile strength of glass may be twice as much as the static tensile strength, when the loading duration is as short as 10 μs. In the impact problem studied here, the loading duration is approximately of 30 μs [12]. It means that the use of a maximum stress failure criterion in this dynamic situation is questionable. A cumulative damage model presented by Tuler and Butcher [14] and Brown [15], which accounts for the variation of material strength with respect to loading duration, is adopted in this paper. Beason and Morgan [19] and Norville and Minor [20] used a simplified version of Brown's [15] expression to model the failure of monolithic glass plates under lateral wind pressure. Damage at the impact site results from high compressive stress during impact. Based on the cumulative damage theory [14, 15], a damage factor K_d is introduced

$$K_\mathrm{d} = \int_0^{t_\mathrm{f}} \Phi\, \mathrm{d}t \tag{8}$$

where t_f is the failure time, t is the time after impact, and the integrand Φ in the damage factor function is defined as

$$\Phi = \begin{cases} \left(\dfrac{\sigma_{\max} - \sigma_0}{\sigma_0}\right)^n & \text{if } \sigma_{\max} \geq \sigma_0 \\ 0 & \text{if } \sigma_{\max} < \sigma_0 \end{cases} \tag{9}$$

in which $\sigma_{\max}$ is the maximum principal compressive stress at the impact site on the exposed surface of the outer glass ply and is a function of the time after impact, σ_0 is the static compressive strength of glass, and n is a material constant to be determined later. According to the usual convention, compressive stresses should take negative values. However, for convenience, both $\sigma_{\max}$ and σ_0 are treated as positive values. Usually, the static compressive strength of glass is taken to be higher than the static tensile strength by as much as 10 to 20 times [18, 21]. For calculations in this paper, the static compressive strength of glass is taken to be 15 times that of the average static tensile strength which is approximately 100 MPa [22], so that $\sigma_0 = 1.5$ GPa. In Equation 8, it is implied that no damage would accumulate at the impact site if the maximum principal compressive stress ($\sigma_{\max}$) is less than the static compressive strength (σ_0). By using finite element stress analysis, $\sigma_{\max}$ is computed as a function of time after impact. Then, the damage factor is computed directly by incorporating an algorithm associated with Equation 8 into the finite element code.

In general, Weibull's probability distribution is very useful for characterizing the probability of failure or damage in glass-like brittle materials [23], which can be expressed as

$$P_\mathrm{d} = 1 - \mathrm{e}^{-B} \tag{10}$$

where P_d is the probability of damage or failure and B is a function that reflects the risk of damage or failure.

Because damage at the impact site (under the impactor) because of high compressive stress is strongly

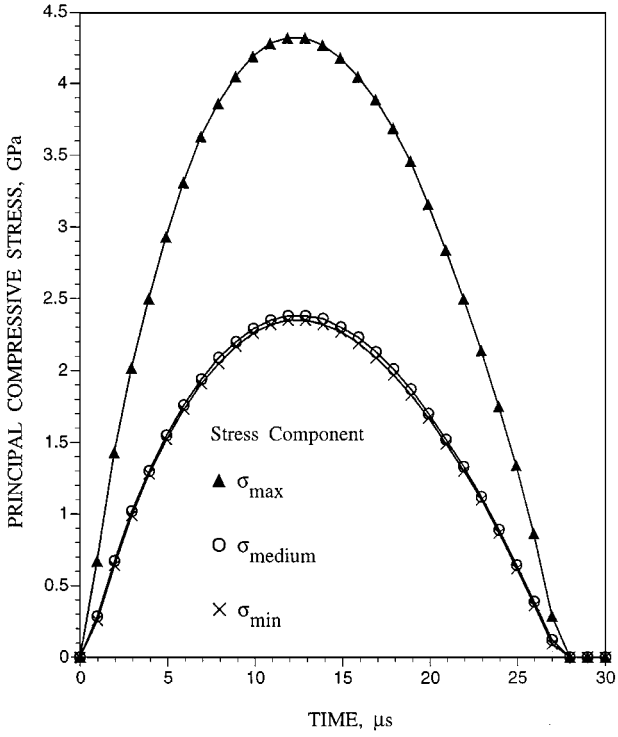

Figure 3 Time history plots of various principal compressive stresses at impact site for a laminated glass unit ($h_o = h_i = 4.81$ mm and $h_{PVB} = 1.52$ mm).

localized, it is unnecessary to relate the risk function B to an integral with respect to the surface area of the laminated glass unit. In addition, because the maximum principal compressive stress at the impact site is much higher than other two principal compressive stresses, as shown in Fig. 3, multi-axial stress correction factor to the risk function B is not necessary. Therefore, in the spirit of Beason and Morgan [19] and Norville and Minor [20], it is assumed that the risk function is related only to the damage factor at the impact site as follows

$$B = \left(\frac{K_d}{K_0}\right)^m \tag{11}$$

where m and K_0 are material parameters to be determined experimentally. The above assumption will be shown later to be reasonable by using controlled experiments in conjunction with the finite element analysis.

The probability of damage at the impact site can be related to the damage factor by substituting Equation 11 into Equation 10 as follows

$$P_d = 1 - \exp\left[-\left(\frac{K_d}{K_0}\right)^m\right] \tag{12}$$

As K_d can be computed directly in the dynamic finite element analysis for any laminated glass unit for any impact velocity, the probability of damage at the impact site can be predicted with respect to impact velocity, glass ply thickness and interlayer thickness by using Equation 12.

2.3. Determination of material parameters

In order to determine the material parameters n, m and K_0 appearing in Equations 9 and 11, Equation 12 is first rearranged as follows

$$\ln\left[\ln\left(\frac{1}{1-P_d}\right)\right] = m\ln K_d - m\ln K_0 \tag{13}$$

From the above equation, $\ln\{\ln[1/(1-P_d)]\}$ varies linearly with respect to $\ln K_d$, while m is the slope and $m(\ln K_0)$ is the intercept. Therefore, by obtaining a plot of $\ln\{\ln[1/(1-P_d)]\}$ versus $\ln K_d$, the material constants m and K_0 can be determined. First, the probability of damage (P_d) at various values (N) of the impact velocity (V_0) for a given laminated glass unit is obtained by controlled impact tests. Then, the damage factor (K_d) is computed at various impact velocities (V_0) for the above laminated glass unit by using the results of the finite element analysis via Equations 8 and 9. At a given impact velocity $V_0^{(i)}$, let $P_d^{(i)}$ correspond to $K_d^{(i)}$ with $i = 1, 2, \ldots, N$. Using the least square method, Equation 13 is fitted through N data points. The summation of the square of the error, R^2, is then given by

$$R^2 = \sum_{i=1}^{N}\left\{\ln\left[\ln\left(\frac{1}{1-P_d^{(i)}}\right)\right] - m\ln K_d^{(i)} + m\ln K_0\right\}^2 \tag{14}$$

Minimizing R^2 with respect to m and $m(\ln K_0)$ leads to the following equations

$$\sum_{i=1}^{N}\ln K_d^{(i)}\left\{\ln\left[\ln\left(\frac{1}{1-P_d^{(i)}}\right)\right] - m\ln K_d^{(i)} + m\ln K_0\right\} = 0 \tag{15}$$

$$\sum_{i=1}^{N}\left\{\ln\left[\ln\left(\frac{1}{1-P_d^{(i)}}\right)\right] - m\ln K_d^{(i)} + m\ln K_0\right\} = 0 \tag{16}$$

Solving the above two equations for m and $\ln K_0$

$$m = \left(\sum_{i=1}^{N}\ln K_d^{(i)}\sum_{i=1}^{N}\ln\left[\ln\left(\frac{1}{1-P_d^{(i)}}\right)\right] - N\sum_{i=1}^{N}\left\{\ln K_d^{(i)}\ln\left[\ln\left(\frac{1}{1-P_d^{(i)}}\right)\right]\right\}\right) \Bigg/ \left[\left(\sum_{i=1}^{N}\ln K_d^{(i)}\right)^2 - N\sum_{i=1}^{N}\left(\ln K_d^{(i)}\right)^2\right] \tag{17}$$

$$\ln K_0 = \left(\sum_{i=1}^{N} \left(\ln K_d^{(i)} \right)^2 \sum_{i=1}^{N} \left\{ \ln \left[\ln \left(\frac{1}{1 - P_d^{(i)}} \right) \right] \right\} - \sum_{i=1}^{N} \ln K_d^{(i)} \sum_{i=1}^{N} \left\{ \ln K_d^{(i)} \ln \left[\ln \left(\frac{1}{1 - P_d^{(i)}} \right) \right] \right\} \right) \Bigg/$$
$$\left(\sum_{i=1}^{N} \ln K_d^{(i)} \sum_{i=1}^{N} \ln \left[\ln \left(\frac{1}{1 - P_d^{(i)}} \right) \right] - N \sum_{i=1}^{N} \left\{ \ln K_d^{(i)} \ln \left[\ln \left(\frac{1}{1 - P_d^{(i)}} \right) \right] \right\} \right) \quad (18)$$

Substituting Equations 16 and 17 into Equation 13, R^2 can be calculated as

$$R^2 = \sum_{j=1}^{N} \left\{ \ln \left[\ln \left(\frac{1}{1 - P_d^{(j)}} \right) \right] - \left[\left(\sum_{i=1}^{N} \left[\ln K_d^{(i)} \ln K_d^{(j)} - \left(\ln K_d^{(i)} \right)^2 \right] \right) \Bigg/ \right.$$
$$\left(\left(\sum_{i=1}^{N} \ln K_d^{(i)} \right)^2 - N \sum_{i=1}^{N} \left(\ln K_d^{(i)} \right)^2 \right) \Bigg] \sum_{i=1}^{N} \ln \left[\ln \left(\frac{1}{1 - P_d^{(j)}} \right) \right]$$
$$+ \left[\left(N \ln K_d^{(j)} - \sum_{i=1}^{N} \ln K_d^{(i)} \right) \sum_{i=1}^{N} \left\{ \ln K_d^{(i)} \ln \left[\ln \left(\frac{1}{1 - P_d^{(i)}} \right) \right] \right\} \right] \Bigg/$$
$$\left. \left[\left(\sum_{i=1}^{N} \ln K_d^{(i)} \right)^2 - N \sum_{i=1}^{N} \left(\ln K_d^{(i)} \right)^2 \right] \right\} \quad (19)$$

Note from Equation 9 that the damage factor K_d is a function of n. Therefore, m, K_0 and R^2 are dependent on n. Generally, n can be chosen to minimize R^2.

3. Results and discussion

First, a series of controlled impact tests were conducted to establish the probability of damage P_d at various impact velocities. Square (305 mm × 305 mm) laminated glass specimens were glazed in a custom-built wood holding frame with rubbber spacers and were simply supported along their entire perimeters. A compressed air cannon was used to propel a 2 g steel ball of 7.94 mm diameter. All impacts were made normal to the outer glass ply with a cannon-to-glass distance of 25 mm, which made velocity loss between the cannon muzzle and the impact site negligible. Details of experimental procedure and description of the apparatus are reported in Behr and Kremer [9]. Fig. 4 shows the experimental results of damage probability (P_d) as a function of impact velocity (V_0) for a laminated glass unit with $h_o = h_i = 4.81$ mm and $h_{PVB} = 1.52$ mm subjected to 2 g steel ball impacts. These experimental results will be used later to determine the material parameters n, m and K_0.

The dynamic finite element analysis was also carried out for the above laminated glass unit ($h_o = h_i =$ 4.81 mm and $h_{PVB} = 1.52$ mm) subjected to 2 g missile impacts at various velocities. Fig. 5 illustrates the computed damage factor at the impact site (K_d) by using Equations 8 and 9 as a function of the impact velocity for various values of n. As expected, the damage factor increases monotonously with the impact velocity for a given value of the material parameter n. It is found that all curves cross over at an impact velocity of 3.5 m s^{-1}. For a fixed impact velocity, the computed damage factor at the impact site K_d decreases with increasing n

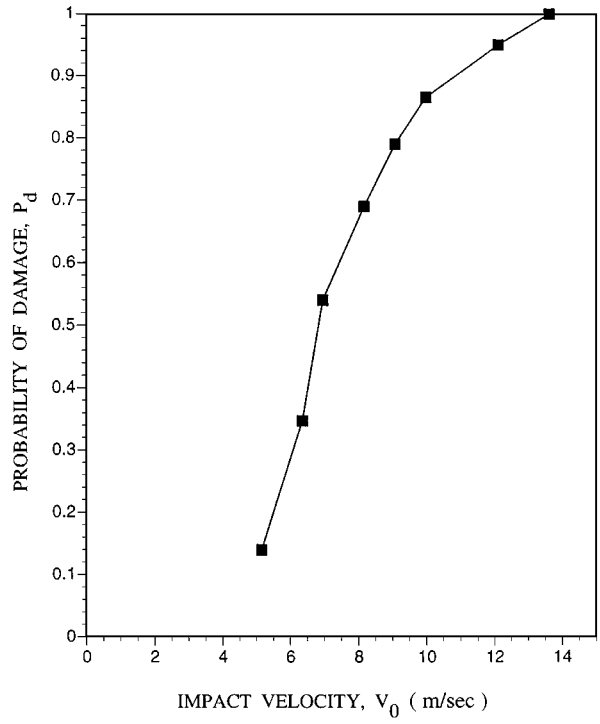

Figure 4 Observed damage probability at various impact velocities for a laminated glass unit ($h_o = h_i = 4.81$ mm and $h_{PVB} = 1.52$ mm).

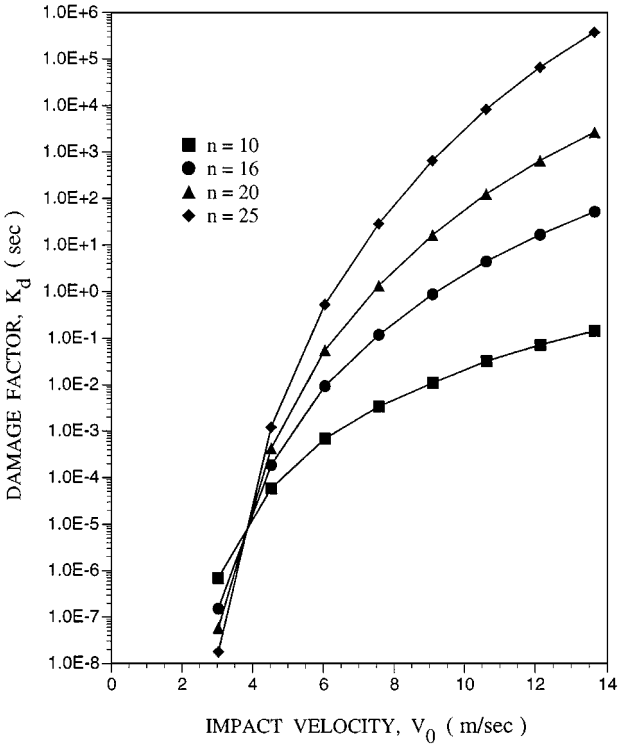

Figure 5 Computed damage factor as a function of impact velocity for various values of n for a laminated glass unit ($h_o = h_i = 4.81$ mm and $h_{PVB} = 1.52$ mm).

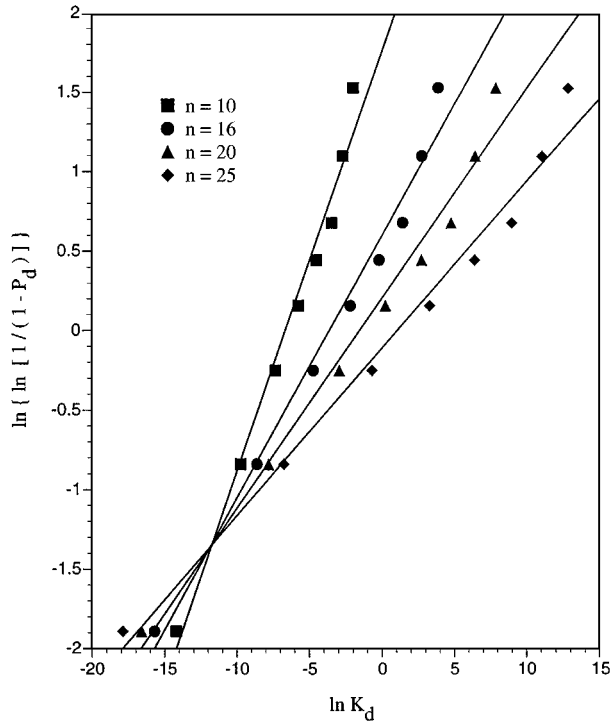

Figure 6 Relationship between damage probability and damage factor for various values of n for a laminated glass ($h_o = h_i = 4.81$ mm and $h_{PVB} = 1.52$ mm).

when the impact velocity is less than 3.5 m s^{-1}, while it increases with increasing n when the impact velocity is higher than 3.5 m s^{-1}.

By combining the results of Figs 4 and 5 at a given impact velocity, the relationship between the probability of damage (P_d) and the damage factor (K_d) for a given value of n is obtained as shown in Fig. 6. It is found that $\ln\{\ln[1/(1 - P_d)]\}$ varies almost linearly with respect to $\ln K_d$ for a given n. Equation 13 is thus validated by experimental data, in conjunction with the finite element analysis. This also implies that all the assumptions made in arriving at Equation 13 are valid.

Having determined P_d and K_d, the material parameters m and K can now be obtained using Equations 17 and 18 for a given n. The variation of the material parameter m as a function of n is shown in Fig. 7. The material parameter m sharply decreases with an increasing n. Fig. 8 shows the variation of the material constant K_0 as a function of n. The logarithm of the material constant K_0 increases approximately linearly with n. For a given value of n, the material constants m and K_0 can be determined by using Figs 7 and 8.

By using Equation 19 and data shown in Fig. 6, the summation of the square of the error (R^2) is calculated to be approximately constant for all values of n used in the analysis, indicating a good fit through the entire range of n values. This finding can be further verified by using the computed damage factor K_d for different values of n from Fig. 5 in Equation 12 to calculate the probability of damage (P_d). Table I shows the predicted probability of damage as a function of n for a given impact velocity. From Table I, it can be seen that the selection of n has no effect on the predicted results. In the following prediction, an arbitrary value $n = 16$ will be used. From Figs 7 and 8, the corresponding material parameters are given by $m = 0.165$ and $K_0 = 2.85 \times 10^{-2}$ s.

TABLE I Effect of selection of n on predicted probability of damage

	Predicted probability of damage, P_d			
V_0 (m s^{-1})	$n = 10$ $m = 0.263$ $K_0 = 1.36 \times 10^{-3}$ s	$n = 16$ $m = 0.165$ $K_0 = 2.85 \times 10^{-2}$ s	$n = 20$ $m = 0.132$ $K_0 = 0.227$ s	$n = 25$ $m = 0.105$ $K_0 = 3.02$ s
3.04	0.127	0.126	0.126	0.128
4.56	0.355	0.354	0.354	0.356
6.08	0.567	0.565	0.565	0.566
7.6	0.720	0.719	0.718	0.718
9.12	0.829	0.829	0.828	0.828
10.64	0.900	0.901	0.900	0.900
12.16	0.943	0.944	0.943	0.943
13.68	0.968	0.969	0.969	0.969

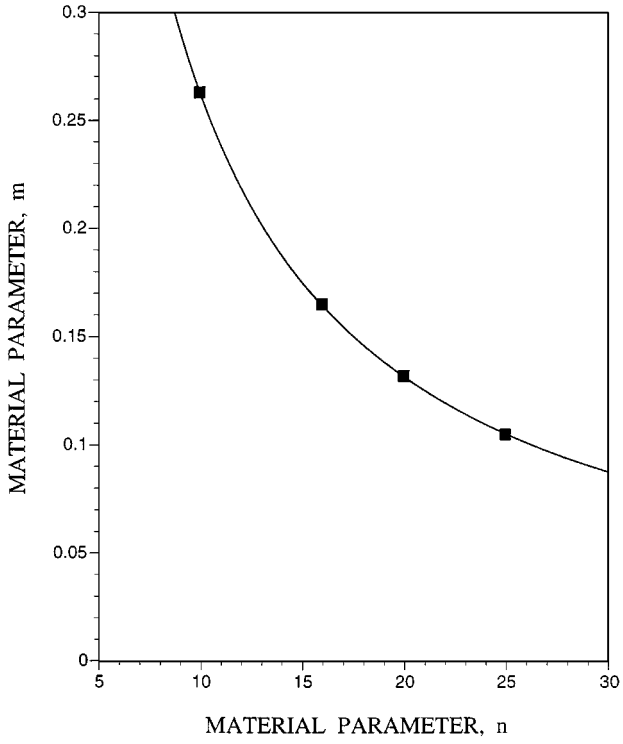

Figure 7 Material parameter *m* as a function of material parameter *n*.

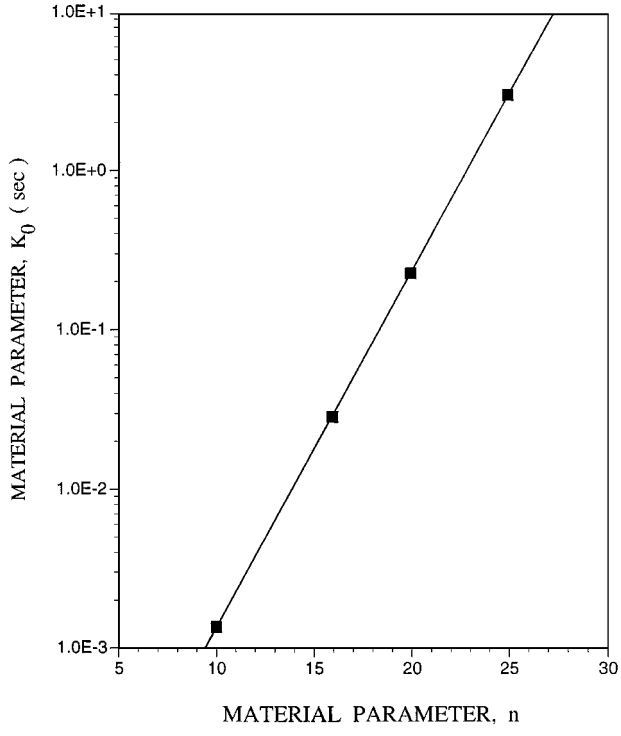

Figure 8 Material parameter K_0 as a function of material parameter *n*.

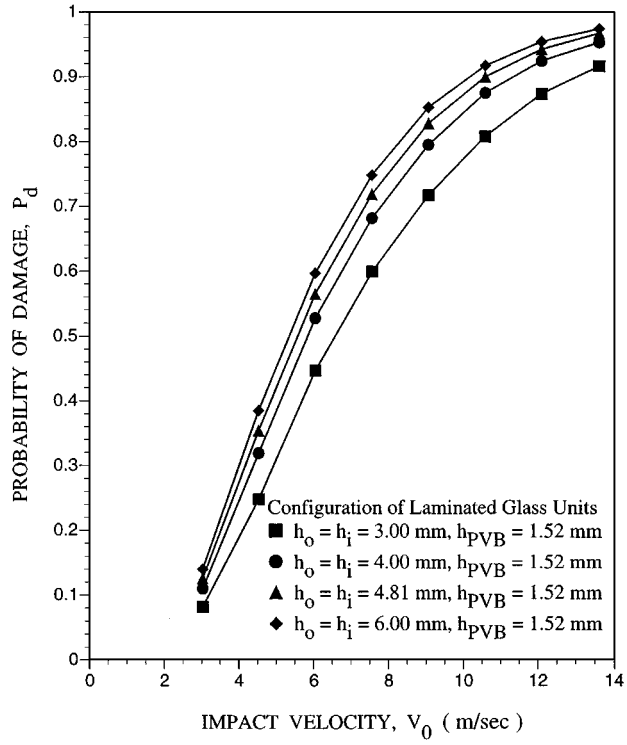

Figure 9 Predicted probability of damage at impact site as a function of impact velocity for different laminated glass units with a fixed PVB interlayer thickness.

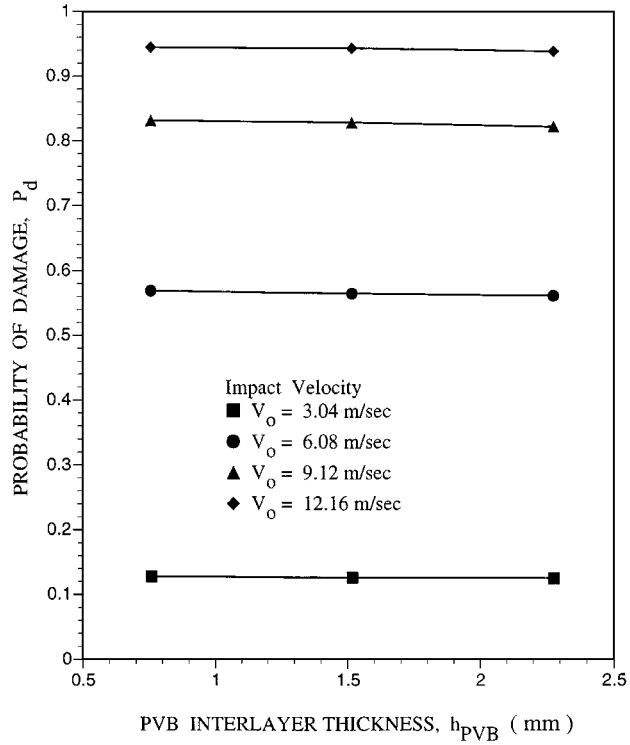

Figure 10 Predicted probability of damage at impact site as a function of PVB interlayer thickness for laminated glass units with $h_0 = h_i = 4.81$ mm.

Fig. 9 illustrates the predicted probability of damage at the impact site in the outer glass ply as a function of the impact velocity for laminated glass units with different glass ply thicknesses but a fixed PVB interlayer thickness. The probability of damage increases as the impact velocity increases for a given glass ply thickness. The probability of damage increases as the impact velocity increases for a given glass ply thickness. For a fixed impact velocity, the probability of damage slightly increases as the glass ply thickness increases.

Fig. 10 shows the predicted probability of damage at the impact site in the outer glass ply as a function of the PVB interlayer thickness for laminated glass units with $h_0 = h_i = 4.81$ mm subjected to 2 g missile impacts at a fixed impact velocity. It is found that the PVB interlayer thickness has a negligible effect on the probability of

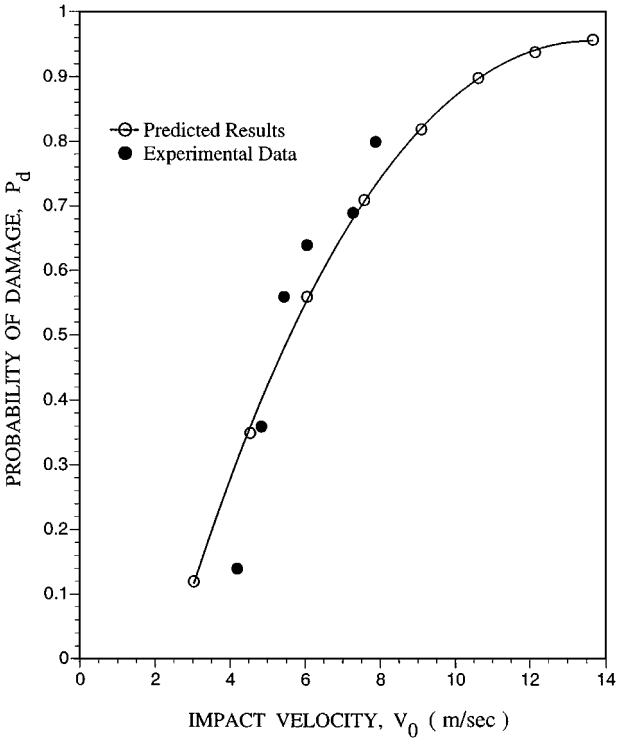

Figure 11 Comparison of prediction results with experimental data for a laminated glass unit with $h_0 = h_i = 4.78$ mm and $h_{PVB} = 0.76$ mm subjected to a low-velocity 2 g missile impact.

damage at the impact site on the exposed surface of the outer glass ply of laminated glass units.

Another group of impact tests were conducted during this investigation for a laminated glass unit with $h_0 = h_i = 4.78$ mm and $h_{PVB} = 0.76$ mm to validate the analytical model presented in this paper. The experimental procedures and apparatus are same as those used in determining the material constants n, m and K_0. The experimental results are compared with the analytical predictions for the above laminated glass unit, as shown in Fig. 11. It is encouraging to note that the predicted probability of damage at the impact site on the exposed surface of the outer glass ply is in good agreement with those experimentally measured.

4. Conclusions

The analytical model developed in this paper based on the dynamic non-linear finite element method can be used to predict the probability of damage at the impact site (under the impactor) of the outer glass ply of laminated glass units subjected to low-velocity small hard missile impacts. Predicted results are in good agreement with experimental data. The probability of damage at the impact site in the outer glass ply depends strongly on the impact velocity and weakly on the glass ply thickness. The PVB interlayer thickness has a negligible effect on the compressive damage of the outer glass ply.

Acknowledgements

This work is being supported by the US National Science Foundation (Grant No. CMS-9628807), the Missouri Department of Economic Development through the Manufacturing Research and Training Center, the E. I. duPont de Nemours and Company, and the Solutia Inc. Authors would like to thank Dr Joseph Minor for many helpful suggestions during the course of this investigation.

References

1. W. L. BEASON, G. E. MEYERS and R. W. JAMES, *J. Struct. Eng.* **110** (1984) 2843.
2. J. R. HUNTSBERGER, *J. Adhesion* **13** (1981) 107.
3. R. A. BEHR, J. E. MINOR, M. P. LINDEN and C. V. G. VALLABHAN, *J. Struct. Eng.* **111** (1985) 1037.
4. R. A. BEHR, J. E. MINOR and M. P. LINDEN, *ibid.* **112** (1986) 1141.
5. C. V. G. VALLABHAN, J. E. MINOR and S. R. NAGALLA, *ibid.* **113** (1987) 36.
6. C. V. G. VALLABHAN, Y. C. DAS, M. MAGDI, M. ASIK and J. R. BAILEY, *ibid.* **119** (1993) 1572.
7. F. W. FLOCKER and L. R. DHARANI, *Eng. Struct.* **19** (1997) 851.
8. C. P. PANTELIDES, A. D. HORST and J. E. MINOR, *J. Struct. Eng.* **119** (1993) 454.
9. R. A. BEHR and P. A. KREMER, *J. Architect. Eng.* **2** (1996) 95.
10. F. W. FLOCKER and L. R. DHARANI, *J. Mater. Sci.* **32** (1997) 2587.
11. F. W. FLOCKER and L. R. DHARANI, *Struct. Eng. Mech.* **6** (1998) 485.
12. R. A. BEHR, L. R. DHARANI, P. A. KREMER, F. S. JI and N. D. KAISER, *J. Amer. Ceram. Soc.* (in review).
13. A. BALL and H. W. MCKENZIE, *J. De Physique. IV* **4** (1994) 783.
14. F. R. TULER and B. M. BUTCHER, *Int. J. Fract. Mech.* **4** (1968) 431.
15. W. G. BROWN, Publication no. NRC 14372, National Research Council of Canada, Ottawa, Ontario, Canada, 1974.
16. R. G. WHIRLEY, B. E. ENGLEMANN and J. O. HALLQUIST, "DYNA2D, a nonlinear, explicit, two-dimensional finite element code for solid mechanics," User Manual, Lawrence Livermore National Laboratory Report, UCRL-MA-110630, 1992.
17. J. O. HALLQUIST, "Theoretical manual for DYNA3D," Lawrence Livermore National Laboratory, UCRL-52112, 1983.
18. J. MENCIK, "Strength and fracture of glass and ceramics" (Elsevier Publishers, New York, 1992) p. 83 and p. 164.
19. W. L. BEASON and J. R. MORGAN, *J. Struct. Eng.* **110** (1984) 197.
20. H. S. NORVILLE and J. E. MINOR, *Amer. Ceram. Soc. Bull.* **64** (1985) 1467.
21. G. S. PISARENKO, "The structural strength of glasses and sitals" (Naukova Dumka, Kiev, 1979).
22. B. R. LAWN, S. M. WIEDERHORN and H. H. JOHNSON, *J. Amer. Ceram. Soc.* **58** (1975) 428.
23. W. WEIBULL, "A statistical theory of the strength of materials," Ingeniorsvetenskapsakademiens, Handlingar NR151, Stockholm, Sweden, 1939.

Received 24 October 1997
and accepted 15 May 1998